Occurrence of Per- and Polyfluoroalkyl Substances in Europe's Rivers

Abstract

Per- and polyfluoroalkyl substances (PFAS) are synthetic chemicals of global concern due to their persistence, mobility, and toxicity. While numerous studies have investigated PFAS contamination in surface waters, most are limited to local or national scales and are constrained by inconsistent methodologies. Here, we present the first large-scale, year-round assessment of PFAS contamination in European rivers. Seven PFAS were monitored at 280 across 93 distinct rivers and 31 countries, representing the PFAS footprint of approximately 309 million people. At least one PFAS was found at 93% of locations, with concentrations at 63% of locations exceeding the EU's proposed environmental quality standard for PFAS of 4.4 ng/L. Hotspots of PFAS contamination included sites in southern and southeastern Europe (e.g., Cyprus and Turkey) and western Europe (e.g., Scotland and France), with contamination associated with landfills, wastewater discharges, and industrial activity. Seasonal trends revealed significantly higher PFAS concentrations in summer, likely due to reduced dilution. Partial least squares path modelling (PLS) showed that PFAS levels were influenced by both socioeconomic factors (e.g., Human Footprint Index and GDP) and environmental conditions (e.g., electrical conductivity, temperature, and flow rate). These findings highlight the need for coordinated monitoring, stronger regulation, and global action to address PFAS pollution and safeguard human and ecosystem health.

1. Introduction

Per- and polyfluoroalkyl substances (PFAS) are a class of synthetic compounds that have been extensively used in industrial and manufacturing processes and incorporated into a wide array of consumer products for decades (Key et al., 1997; Buck et al., 2011). Characterized by the exceptional strength of their carbon-fluorine bonds, PFAS exhibit resistance to biological and chemical degradation, earning them the moniker "forever chemicals" (Buck et al., 2011; Cousins et al., 2020). The persistent, mobile, and bioaccumulative nature of PFAS, coupled with their widespread use, has resulted in their widespread presence in aquatic environments, including in drinking water supplies and food chains (Shi et al., 2015; Chen et al., 2016; Camacho et al., 2024; Becker et al., 2008; Reinikainen et al., 2022). Human exposure to PFAS has been associated with severe health risks, including increased cancer incidence, liver toxicity, immune system suppression, and endocrine disruption in humans (Pizzurro et al., 2019; Messmer et al., 2022). Additionally, PFAS pose acute and chronic toxicity risks to aquatic species, threatening ecosystem integrity (Sinclair et al., 2020; Wang et al., 2024). Consequently, the global scientific and regulatory community recognizes PFAS contamination as a critical threat to both human health and environmental systems.

In response to these concerns, regulatory frameworks have been established to mitigate PFAS risks. For example, the European Commission implemented an annual average environmental quality standard (AA-EQS) of 0.65 ng/L for perfluorooctane sulfonate (PFOS) in 2013 and subsequently proposed a broader AA-EQS of 4.4 ng/L for a group of 24 PFASs in surface and groundwater, expressed as perfluorooctanoic acid (PFOA) equivalents (European Union, 2013; European Commission, 2022). Similar thresholds have been adopted internationally, including drinking water limits of 4 ng/L for PFOS and PFOA, and 10 ng/L for PFNA in the United States (US EPA, 2023). The European Union Drinking Water Directive defines a threshold of 0.1 µg/L for a group of twenty PFASs (European Union, 2020). Despite these regulatory measures, there remain significant gaps in our understanding of PFAS distribution and trends in environmental systems, particularly at broader spatial and temporal scales.

Although numerous studies have examined the occurrence of PFAS in surface waters and groundwaters, most have focused on small sample sizes or limited geographic regions, such as single basins or countries (Camacho et al., 2024; Zarębska et al., 2024; Sörengård et al., 2022; Jonker, 2024). Large-scale assessments of PFAS distribution are rare, with only three studies to date investigating continental or global patterns in occurrence (Pan et al., 2018; Baabish et al., 2021; Loos et al., 2009). These efforts covered just 158 surface water samples across 27 European countries and lacked the temporal resolution necessary to assess variations over time. While desk-based studies have aggregated data from multiple sources to examine PFAS contamination at continental and global scales (Ackerman Grunfeld et al., 2024), inconsistencies in analytical methods and monitoring protocols hinder cross-study data integration and interpretation. Recent mapping efforts by Cordner et al. (2024) have identified likely PFAS contamination hotspots across Europe by analysing potential source categories. However, the reported contamination levels may underestimate the true extent of PFAS pollution due to national disparities in monitoring capacity, data transparency, and a lack of comprehensive geolocation and sampling data. To address these limitations, spatially representative environmental monitoring data, generated using standardized and coordinated sampling and analytical protocol, are essential for accurately characterising the general extent of PFAS contamination across Europe.

In this study, we address these critical gaps by presenting the first comprehensive assessment of the spatial and temporal distribution of seven widely detected PFAS across freshwater systems in 31 European countries. By analyzing data from 280 monitoring sites, we identify key drivers of PFAS distribution, assess contamination hazards, and pinpoint European hotspots of PFAS pollution. Our findings provide crucial insights to inform regulatory strategies and advance efforts to mitigate PFAS contamination at a continental scale.

2. Materials and Methods

2.1 Study PFAS and reagents

Four short-chain PFAS, including perfluorohexanoic acid (PFHxA), perfluorobutanesulfonic acid (PFBS), perfluoroheptanoic acid (PFHpA), and perfluorobutanoic acid (PFBA), and three long-chain PFAS, including perfluorooctanoic acid (PFOA), perfluorononanoic acid (PFNA), and perfluorooctanesulfonic acid (PFOS), were selected for monitoring based on their high detection frequencies (ranging from 17% (PFNA) to 42% (PFOS)), and mean environmental concentrations (ranging from 0.820 ng/L (PFNA) to 68.3 ng/L (PFBA)) across 1191 aquatic monitoring sites in Europe (Niegowska et al., 2021). The seven target chemical standards and the deuterated internal standard (atrazine-D5) were purchased from Sigma-Aldrich (Gillingham, UK) with a purity of ≥95%. LC-MS grade water, methanol, and acetonitrile were obtained from Fisher Scientific (Loughborough, UK). Ammonium formate (≥97%) and formic acid (≥95%) were purchased from Sigma-Aldrich (Gillingham, UK).

2.2 Site selection and sampling protocol

Sampling locations were strategically chosen to characterize PFAS occurrence from a range of potential pollution sources, such as industrial discharges, wastewater treatment plants, and agricultural runoff, as well as to include reference sites expected to be uncontaminated. The final sites were selected based on criteria including river size, setting (urban or rural), and land

use (e.g., industrial or agricultural areas) to ensure a representative assessment of PFAS contamination across the European landscape. A total of 280 river water sampling locations across 31 countries on the European continent were monitored. The number of locations by country ranged from 3 for Estonia to 54 for the United Kingdom. Full details of the sampling locations are provided in Supporting Information (Table S1).

The sampling approach was similar to that described by Wilkinson et al. (2022). Duplicate samples were collected from each sampling location in the summer (July) and autumn (October) of 2022, and winter (January) and spring (April) of 2023. All samples for a season were obtained within a one-month timeframe of each other (sampling dates for each location are provided in the Supporting Information, Table S1). Samples were collected using a pre-rinsed metal bucket. An aliquot of the water was then drawn into a 5 ml disposable plastic syringe, and 3 mL was filtered using a 0.45 µm glass microfiber (GFX) filter into 4 mL amber glass vials. For each sampling campaign and each sampling timepoint, a field blank was collected following a procedure similar to that used for environmental samples but using LCMS-grade water instead of river water. The collected samples were frozen and transported on ice to the University of York (York, UK) for chemical analysis. All shipments were sent via the international DHL Express 12:00 service and arrived within 24–72 hours after dispatch. General water quality parameters (e.g., pH, water temperature, electrical conductivity, and flow rate) were measured when meters were available to sampling teams.

2.3 Chemical analysis

Concentrations of each PFAS in samples were determined using direct-injection high-performance liquid chromatography-tandem mass spectrometry (HPLC-MS/MS) in multiple reaction monitoring mode. The HPLC-MS/MS system consisted of a Dionex UltiMate 3000 HPLC coupled with a Thermo Scientific Endura TSQ triple-quadrupole mass spectrometer. Chromatographic separation was performed using an Agilent Zorbax Eclipse Plus C18 column (3.0 × 100 mm, 1.8 µm, 600 bar, Agilent Technologies, UK) with a C18 SecurityGuard guard column (Phenomenex, UK). The column temperature was maintained at 40°C, with a mobile phase flow rate of 0.45 mL/min. Mobile phase A consisted of 0.01 M formic acid and 0.01 M ammonium formate in LCMS-grade water, while mobile phase B was 90% methanol and 10% acetonitrile. The sample injection volume was 100 µl. Gradient elution began at 10% B, increased to 40% at 5 min, 60% at 10 min, and 100% at 14.1 min, then held for 2 min before returning to 10% at 16.1 min, followed by a 1.4-min re-equilibration. Negative electrospray ionization was used to generate two transition ions per target PFAS, while positive ionization was used for the internal standard (atrazine-D5), with one transition for quantification and the other for confirmation. Collision gas (argon) pressure was kept at 2 mTorr. Further details on analytical methods are provided in Table S2.

Quantification was performed using a 15-point calibration curve (1–8000 ng/L) with TraceFinder 5.1 software (Thermo Scientific, Waltham, MA, USA). Limits of detection (LOD) and quantification (LOQ) were determined following Wilkinson et al. (2019). The LOD for each analyte was calculated as the standard deviation of 8 replicate measurements at the lowest calibrant level, multiplied by the Grubbs t-test constant. LOQs were set at twice the corresponding LOD. The LODs for the seven PFAS compounds ranged from 0.960 ng/L for PFOA to 1.76 ng/L for PFOS (Table S3). The proposed method achieved good intra- and inter-day repeatability in LCMS-grade water at spiking concentrations of 100 and 1000 ng/L (n = 8), with relative standard deviations below 20% for all target PFAS. Matrix recovery was tested by spiking filtered river water (River Foss, York, UK) at the same concentrations (100 and 1000

ng/L), with recoveries ranging from 83% (PFBA) to 137% (PFNA) (Table S3). A QC blank (LCMS-grade water spiked with an internal standard at 400 ng/L) and an instrument quality control sample (LCMS-grade water spiked with all target PFAS, including the internal standard, at 800 ng/L) were injected after every 20 samples during the analytical runs to evaluate sample contamination throughout the analytical procedures and monitor the performance of the HPLC-MS/MS. Alongside field blanks, method blanks (with vials rinsed with LCMS-grade water and subjected to the same filtration procedure as field blanks), and laboratory blanks (prepared with LCMS-grade water spiked with an internal standard) were analyzed to assess background and carryover contamination and validate the sample preparation process.

2.4 Statistical Analysis

Data were compiled in and managed using Microsoft Excel (Microsoft 365, Version 2412, USA). PFAS that were not detected or detected at concentrations below the LOD were reported as not detected (ND).

With the exception of PFHxA, for statistical analysis of the data and in the event that compounds were not detected, a value of zero was used in subsequent data analyses. For PFHxA, which had a detection frequency exceeding 60%, non-detects were substituted using the approach described by Antweiler (2015) and calculated according to Equation 1.

$$Substitution = \frac{\sqrt{2}}{2} \times LOD$$

Figures displaying the spatial and temporal distribution of PFAS concentrations were generated using GraphPad Prism 9 (GraphPad Software, 2020). A hazard characterisation map was created in RStudio Version 4.4.2 (RStudio, 2024) by comparing the measured PFAS concentrations against European regulatory PFAS thresholds for surface water (European Union, 2013; European Commission, 2022). Given the non-normal distributions of individual PFAS, total PFAS concentrations, and hazard quotients, a non-parametric two-way ANOVA with the aligned rank transform function (ARTool package) was conducted in RStudio Version 4.4.2 (RStudio, 2024) to assess significant differences in total PFAS concentration between countries and across the four seasons. Additionally, a non-parametric Friedman test was performed in GraphPad Prism 9 (GraphPad Software, 2020) to determine whether individual PFAS concentrations or hazard quotients differed significantly across the four seasons; this was followed by Dunn's multiple comparisons test to identify specific pairwise seasonal differences. For detection frequencies of individual PFAS, Cochran's Q test was used to assess overall seasonal differences, followed by McNemar's test to determine significant pairwise seasonal differences. The significance threshold in all statistical analyses was $p < 0.05$.

Partial least squares path modelling (PLS-PM) was also conducted in RStudio Version 4.4.2 (RStudio, 2024) to identify key contributors among socioeconomic and environmental factors that might explain spatial and temporal variations in PFAS concentrations. PLS-PM consists of an inner model, which describes the relationships between the dependent variable ('PFAS concentration') and latent variables (LVs), such as 'socioeconomic variables' and 'environmental variables,' and an outer model, which links the measurement variables (MVs) to their corresponding LVs. All data were square root-transformed to approximate a normal distribution and subsequently standardized to ensure variable comparability in the PLS-PM analysis. The relative contribution and significance of both LVs and MVs were evaluated using the bootstrapping method. The weights and path coefficients range from −1 to 1, with values

closer to −1 or 1 indicating stronger relationships, and those closer to zero representing weaker relationships.

Socioeconomic data at the regional level, including population, gross domestic product (GDP), education, poverty, land use and tourism, at the Nomenclature of Territorial Units for Statistics Level 2 (NUTS2), were obtained from the Eurostat database for 2022–2023 (Eurostat, 2024). When region-specific data for 2022–2023 were unavailable, data from the nearest available year were used. Additional socioeconomic data on manufacturing of all types of pollutants, wastewater treatment plants (WWTPs), and the Human Footprint Index (HFI) were sourced from the European Environment Agency (EEA, 2024a), HydroWASTE (Ehalt Macedo et al., 2022), and the study by Mu et al. (2022), with priority given to upstream data of the sampling sites, as upstream activities are likely to most significantly impact PFAS contamination at the monitoring sites.

Environmental condition variables, such as pH, electrical conductivity, water temperature, dissolved organic carbon (DOC), air temperature, precipitation, and flow rate, were derived from either the direct coordinates of the sampling sites or the mean values for the upstream catchment. The upstream catchment was delineated using the 30-arc-second (~1 km) directional flow raster provided by HydroSHEDS (Lehner and Grill, 2013). Environmental properties, including pH, electrical conductivity, and water temperature, were obtained from onsite measurements (Table S4). Missing data were supplemented using extracted data from FOREGS (Salminen et al., 2005) for pH, and electrical conductivity, TerraClimate (Abatzoglou et al., 2018) for water temperature. Additional environmental data, including DOC from FOREGS, air temperature and precipitation from TerraClimate, and flow rate from FLO1K (Barbarossa et al., 2018), were also incorporated into the analysis. Spatial data extraction and processing were performed in R version 4.4.2 with the terra (1.7.65), exactextractr (0.10.0), and sf (1.0-15) packages. Any remaining missing data for socioeconomic and environmental variables were imputed using the k-Nearest Neighbors (kNN) algorithm implemented in the VIM (6.3.2) package. Prior to PLS-PM, a two-tailed Spearman correlation analysis was conducted on descriptors of latent variables within and between groups in GraphPad Prism 9 (GraphPad Software, 2020) to minimize collinearity effects on the modelling. Only one variable was retained from each group of highly intercorrelated variables ($r > 0.7$). The details of the PLS-PM variable data are provided in Table S4.

3. Results and Discussion

In total, 2,410 distinct samples were anticipated (280 sites sampled 4 times, including duplicates and 170 field blanks) but only 2,348 samples were eventually analysed, generating 16,436 data points. The remaining 62 samples (2.6%) were not analysed due to either missed sampling at certain sites (e.g., Tübingen, Germany, during summer and autumn) or sample damage upon arrival. Subsequent data analyses are based on the mean of duplicate measurements for each location and season (1089 values in total). Duplicate results were typically within a two-fold range, with a median fold difference of 1.40 (Mean: 1.70; range: 1.00–7.40). Higher deviations were generally observed in samples with very low concentrations, where minor absolute differences can result in larger fold changes. Individual results for these samples, along with associated metadata provided by the sampling teams, are available in the Supporting Information. Six of the seven PFAS compounds were not detected in any blank samples. PFHxA was detected in fewer than 8.9% of field and QC blanks, but always at concentrations below the LOD (0.99 ng/L), and was therefore treated as

non-detected and assigned a value of zero for statistical analysis. In summary, no PFAS were found in blank samples at quantifiable levels.

3.1 General findings

At least one of the studied PFAS was detected in 775 out of 1089 (71%) of the field samples analysed and at 260 (93%) of the 280 locations that were monitored. The most frequently detected study compound was PFHxA which was detected at 52% of locations, followed by PFOA (43%), PFBS (19%), PFNA (16%), PFBA (5.1%), PFOS (2.0%), and PFHpA (1.6%). Concentrations of the study PFAS ranged from 0.990 (Dalaman, Turkey, summer) to 304 ng/L (Garyllis, Cyprus, autumn) for PFHxA (Mean = 7.24 ng/L), 0.960 (River Liffey, Ireland, spring) to 189 ng/L (Kelvin, Scotland, winter) for PFOA (Mean = 4.55 ng/L), 1.24 (Rhône, France, spring) to 168 ng/L (Garyllis, Cyprus, autumn) for PFBS (Mean = 2.24 ng/L), 4.65 (Thur, Switzerland, spring) to 279 ng/L (Rhône, France, summer) for PFHpA (Mean = 1.24 ng/L), 1.10 (Po, Italy, autumn) to 108 ng/L (Kelvin, Scotland, winter) for PFNA (Mean = 1.18 ng/L), 1.37 (Sana, Bosnia and Herzegovina, summer) to 124 ng/L (Garyllis, Cyprus, autumn) for PFBA (Mean = 0.950 ng/L) and 1.76 (Ringvaart, Belgium, summer) to 67.8 ng/L (Aller, Germany, summer) for PFOS (Mean = 0.231 ng/L). While the concentrations observed for PFHxA, PFHpA, and PFNA were similar to concentrations reported in other European monitoring investigations (Loos et al., 2009; Niegowska et al., 2021), the frequency of detection and average concentrations observed for PFOS and PFOA were both lower. This mismatch might be explained by European regulatory restrictions, including Directive 2006/122/EC (European Union, 2006), which restricted the use of PFOS and its precursors in 2008 and Commission Regulation 2017/1000 (European Commission, 2017), which imposed restrictions on PFOA and its precursors in 2020.

3.2 Most PFAS contaminated and least contaminated sites

The most contaminated site was in Garyllis, Cyprus. This site had an annual mean cumulative PFAS concentration of 408 ng/L, and a maximum concentration of 832 ng/L seen in the autumn. This high cumulative concentration was primarily attributed to PFBA, PFBS, PFHpA, PFHxA, and PFOA. PFNA was only detected in summer, and PFOS was not detected at this site. The site is located downstream of the Vati landfill in the Greater Limassol Area. Elevated PFAS levels at this location may be linked to multiple sources, including partially treated sewage from unlined lagoons, industrial effluent, landfill leachate runoff, and increased sewage flows during summer and autumn, which place additional strain on the treatment capacity.

In Scotland, two sites located in the downstream section of the River Kelvin had the second and third highest annual mean cumulative PFAS concentrations, with 105 ng/L measured at the upper site and 100 ng/L at the lower site. A site on the River Almond ranked fourth, with 97.8 ng/L. The upper site in the downstream section of the River Kelvin is situated approximately 650 metres downstream of the Dawsholm Recycling Centre. In contrast, the lower site is located around 400 metres from Maryhill train station and 2 kilometres from the Glasgow Seaplane Terminal.

A location on the Ergene River in Turkey was ranked fifth with a concentration of 94.3 ng/L driven by PFHxA, PFNA, and PFOA. This location is situated approximately 600 meters downstream of the Lüleburgaz Atıksu Arıtma Tesisi wastewater treatment plant, with upstream flow passing through several Organized Industrial Zones in the Çorlu region. These findings suggest that, in addition to wastewater treatment plants, landfills, recycling centres, and other industrial facilities are significant sources of PFAS pollution. This aligns with the findings of Fernandez et al. (2023), who demonstrated that proximity to known PFAS sources (e.g.,

landfills, airports, and industrial facilities) is a key predictor of contamination levels in drinking water.

Sites with low cumulative PFAS concentrations were typically located in areas with minimal anthropogenic pressure, such as sites within national parks (e.g., Dee, Scotland), upper river reaches (e.g., Úlfarsá in Iceland and Cávado River in Portugal), small towns with low population density (e.g., Vigala, Estonia; Varmá and Ölfusá, Iceland), and locations lacking PFAS sources such as industrial zones or airport facilities within the catchment and upstream region (e.g., Ythan and Tay, Scotland), all of which showed no detectable levels of the seven target PFAS.

3.3 Variation in PFAS occurrence by country

PFAS were detected in river water samples from all 31 monitored countries. In 20 of the monitored countries, PFAS were detected at all sampling sites. In contrast, in Italy, Cyprus, the United Kingdom, Portugal, Slovakia, Latvia, Bulgaria, Slovenia, Poland, Iceland, and Estonia, PFAS were not detected at every site. Belgium exhibited the highest detection frequency (52%), followed by Germany, Austria, France, and the Netherlands, each with detection frequencies exceeding 30%. In contrast, Estonia showed the lowest detection frequency (2.4%). Iceland, Poland, Slovenia, Bulgaria, Latvia, Norway, Slovakia, and Portugal, all had detection frequencies below 10%. Notably, Greece was the only country where all seven target PFAS compounds were detected (Figure 1A). Cyprus had the highest annual average cumulative PFAS concentration, with a value of 73.5 ng/L (Figure 1B). This was followed by Belgium (41.3 ng/L), Luxembourg (40.7 ng/L), the Netherlands (39.5 ng/L), Spain (38.8 ng/L), France (37.9 ng/L), Italy (32.7 ng/L), Greece (32.6 ng/L), and Germany (29.2 ng/L) (Figure 1B). In contrast, Iceland exhibited the lowest concentration (0.528 ng/L), followed by Latvia (1.37 ng/L), Estonia (1.53 ng/L), Bulgaria (1.72 ng/L), Slovakia (3.35 ng/L), Albania (3.98 ng/L), Poland (4.30 ng/L), Slovenia (4.76 ng/L), and Romania (4.80 ng/L), indicating lower PFAS contamination in Eastern and Northern Europe. Some of the countries identified with high average PFAS contamination (i.e., Spain, Germany, and the Netherlands) align with countries recently identified by Zhao et al. (2025), using a combination of monitoring data, risk analysis and machine learning predictions, as being vulnerable to PFAS contamination. In addition, several nationwide monitoring studies have reported comparable PFAS levels in countries with relatively elevated concentrations in this study. For example, Jonker (2024) reported annual average cumulative concentrations of seven PFAS compounds—matching those in our study—of approximately 27 ng/L across 17 inland and coastal sites in the Netherlands in 2022, closely aligning with the 39.5 ng/L we recorded. Similarly, Munoz et al. (2015) reported a mean cumulative concentration of 28 ng/L for 22 PFAS compounds in freshwater samples (n = 333) from 133 rivers and lakes across France in 2013, which is consistent with the 37.9 ng/L we observed.

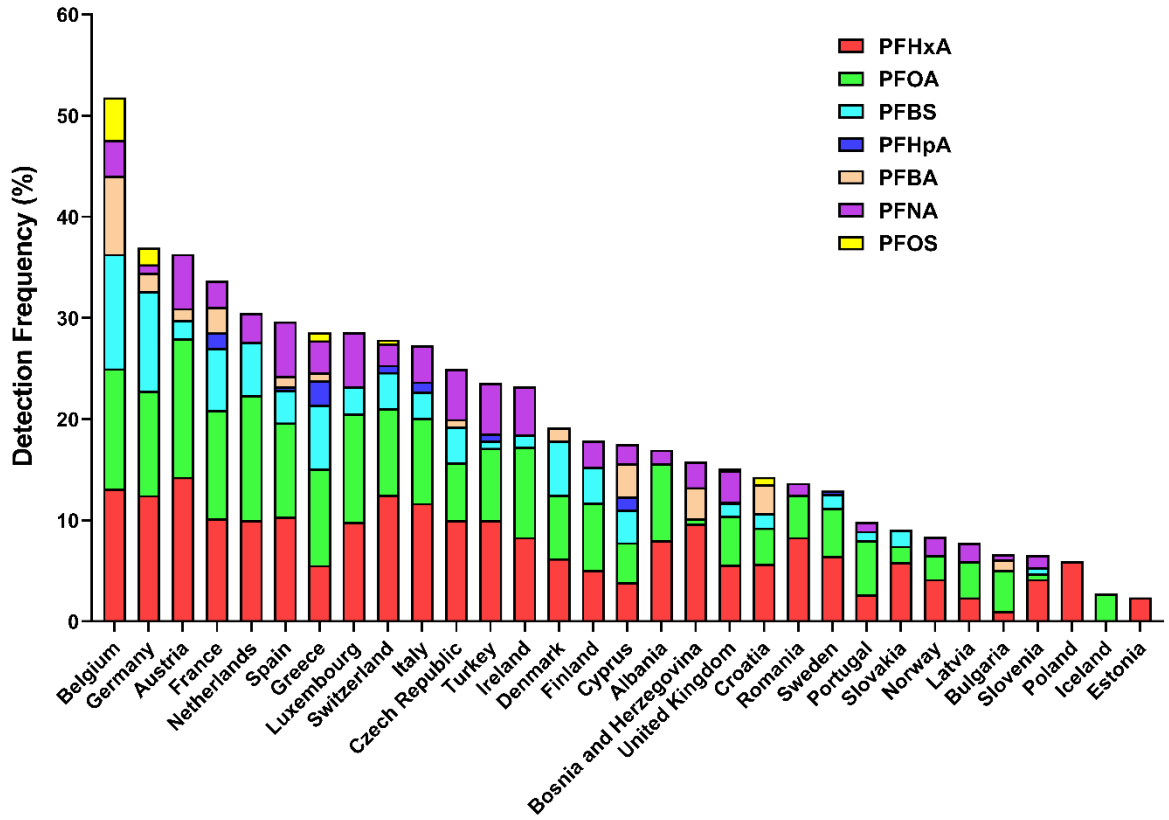
Detection Frequency (%)
60
50
40
30
20
10
0
PFHxA
PFOA
PFBS
PFHpA
PFBA
PFNA
PFOS
Belgium
Germany
Austria
France
Netherlands
Spain
Greece
Luxembourg
Switzerland
Italy
Czech Republic
Turkey
Ireland
Denmark
Finland
Cyprus
Albania
Bosnia and Herzegovina
United Kingdom
Croatia
Romania
Sweden
Portugal
Slovakia
Norway
Latvia
Bulgaria
Slovenia
Poland
Iceland
Estonia

321 (A)

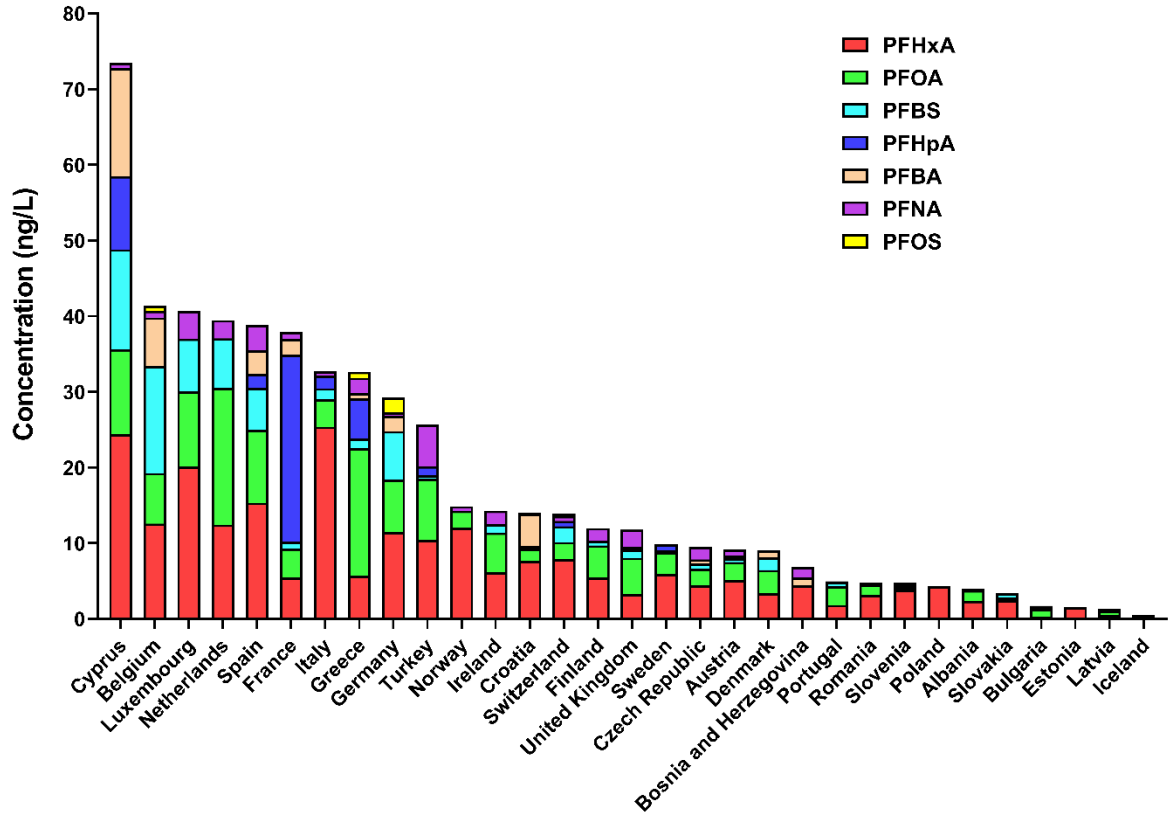
Concentration (ng/L)
80
70
60
50
40
30
20
10
0
PFHxA
PFOA
PFBS
PFHpA
PFBA
PFNA
PFOS
Cyprus
Belgium
Luxembourg
Netherlands
Spain
France
Italy
Greece
Germany
Turkey
Norway
Ireland
Croatia
Switzerland
Finland
United Kingdom
Sweden
Czech Republic
Austria
Denmark
Bosnia and Herzegovina
Portugal
Romania
Slovenia
Poland
Albania
Slovakia
Bulgaria
Estonia
Latvia
Iceland

322 (B)

Figure 1. Summary of PFAS occurrence across 31 European countries: (A) detection frequencies of seven target PFASs, and (B) annual average concentrations, calculated as the mean across all sampling sites within each country. The PFAS acronyms are defined as follows: PFHxA (perfluorohexanoic acid), PFOA (perfluorooctanoic acid), PFBS (perfluorobutanesulfonic acid), PFHpA (perfluoroheptanoic acid), PFBA (perfluorobutanoic acid), PFNA (perfluorononanoic acid), and PFOS (perfluorooctanesulfonic acid).

3.4 Variation in PFAS occurrence by season

Cumulative PFAS concentrations across all countries differed significantly among the four seasons monitored (non-parametric two-way ANOVA, $F = 23.5$, $p < 0.001$). A significant interaction effect between season and country was also observed (non-parametric two-way ANOVA, $F = 2.20$, $p < 0.001$), indicating that seasonal variation in PFAS levels differed among countries. The highest mean cumulative concentration and detection frequency (across 7 PFAS compounds and all sites) were observed in the summer (23.6 ng/L and 24%, respectively), followed by autumn (17.9 ng/L and 20%), winter (16.9 ng/L and 18%), with the spring having the lowest mean cumulative concentrations and detection frequency (12.3 ng/L and 17%), as shown in Figure 2. Seasonal differences in occurrence were also observed for some of the individual PFAS. For PFHxA, both concentrations (Friedman test: statistic = 32.1, $p < 0.001$; Dunn's test: adjusted $p < 0.05$) and detection frequencies (Cochran's Q test: statistic = 12.5, $p < 0.01$; McNemar's test: $p < 0.05$) were significantly higher in summer, autumn, and winter than in spring. For PFBS, concentrations were significantly higher in summer and autumn than in winter, and higher in summer than in spring (Friedman test: statistic = 38.6, $p < 0.0001$; Dunn's test: adjusted $p < 0.05$). Detection frequencies were significantly higher in summer, autumn, and spring compared to winter (Cochran's Q test: statistic = 25.8, $p < 0.001$; McNemar's test: $p < 0.01$). PFNA exhibited significantly higher concentrations in summer than in both spring and autumn (Friedman test: statistic = 26.4, $p < 0.001$; Dunn's test: adjusted $p < 0.05$), with detection frequencies also significantly higher in summer and winter compared to spring and autumn (Cochran's Q test: statistic = 18.4, $p < 0.001$; McNemar's test: $p < 0.05$). For PFOA, both concentrations (Friedman test: statistic = 25.6, $p < 0.001$; Dunn's test: adjusted $p < 0.05$) and detection frequencies (Cochran's Q test: statistic = 22.7, $p < 0.001$; McNemar's test: $p < 0.01$) in summer were significantly higher than in the other three seasons. In contrast, PFBA showed no significant differences in concentration or detection frequency across the four seasons, likely due to low detection frequency (5.1%) and insufficient statistical power. The overall seasonal pattern aligns with the findings of Pignotti et al. (2017), who reported higher PFAS concentrations and detection frequencies in the Ebro River (Spain) during the dry season compared to the wet winter season. This was likely due to reduced dilution and increased detectability associated with lower river flow rates. The higher level of occurrence in the summer may also be attributed to increases in outdoor human activity (Podder et al., 2021), faster transformation of precursor substances (Bertilsson et al., 2013) and/or enhanced inputs to river systems through volatilisation (Zhao et al., 2013; Wang et al., 2009; Shaw et al., 2019).

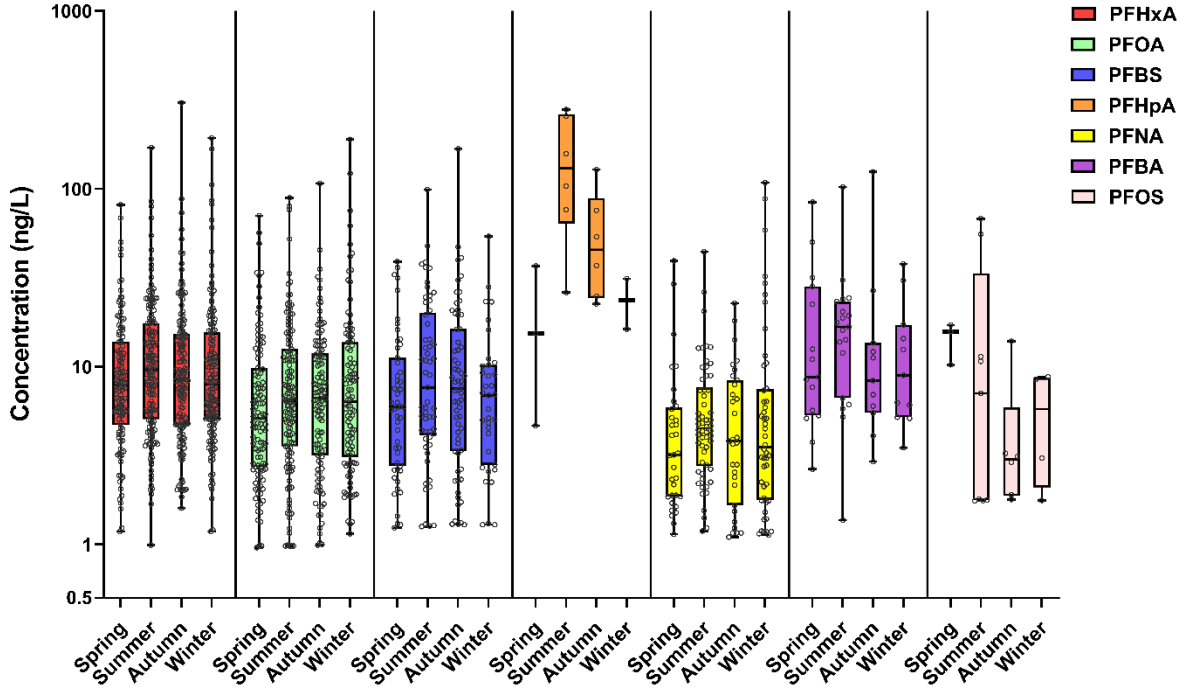

Figure 2. Boxplot of concentrations of seven target PFAS across 280 sampling sites over four seasons. The lower and upper boundaries of the box represent the 25th and 75th percentiles, respectively, while the central line indicates the median concentration, and the whiskers show the minimum and maximum concentrations for each PFAS.

3.5 Partial least squares path modelling to identify drivers of PFAS occurrence

The PLS-PM modelling showed that PFAS concentrations across the study sites were positively associated with socioeconomic factors, including the Human Footprint Index (HFI), Gross Domestic Product (GDP), poverty rate, upstream catchment population density and educational attainment (Figure 3). Environmental variables such as electrical conductivity, temperature, longitude, precipitation and flow rate were also found to be important. The strongest association was seen for HFI (weight = 0.805, $p < 0.001$). This index characterizes human pressures on natural ecosystems using eight criteria: built environment, population density, nighttime lights, cropland, pasture, roads, railways, and navigable waterways (Mu et al., 2022). GDP (weight = 0.384, $p < 0.001$) emerged as the second most important social variable. GDP has been identified as an indicator of the consumption of PFAS-containing products and per capita daily emissions, showing a strong positive correlation with total PFAS concentrations, reflecting higher PFAS contamination in economically developed areas (Calore et al., 2023; Zhang et al., 2013). PFAS pollution was positively associated with the poverty rate (weight = 0.204, $p < 0.001$) and educational attainment (weight = 0.133, $p < 0.001$), consistent with findings by Ayodele and Obeng-Gyasi (2024), who reported that such sociodemographic factors can significantly influence PFAS exposure levels. Upstream catchment population density also exhibited a significant positive relationship (weight = 0.166, $p < 0.001$). This variable was strongly correlated with the number of wastewater treatment plants ($r = 0.820$, $p < 0.05$; Figure S1B) and the total volume of upstream wastewater discharge ($r = 0.840$, $p < 0.05$; Figure S1B), highlighting the role of wastewater as a major source of PFAS contamination, as also confirmed by Lee et al. (2020).

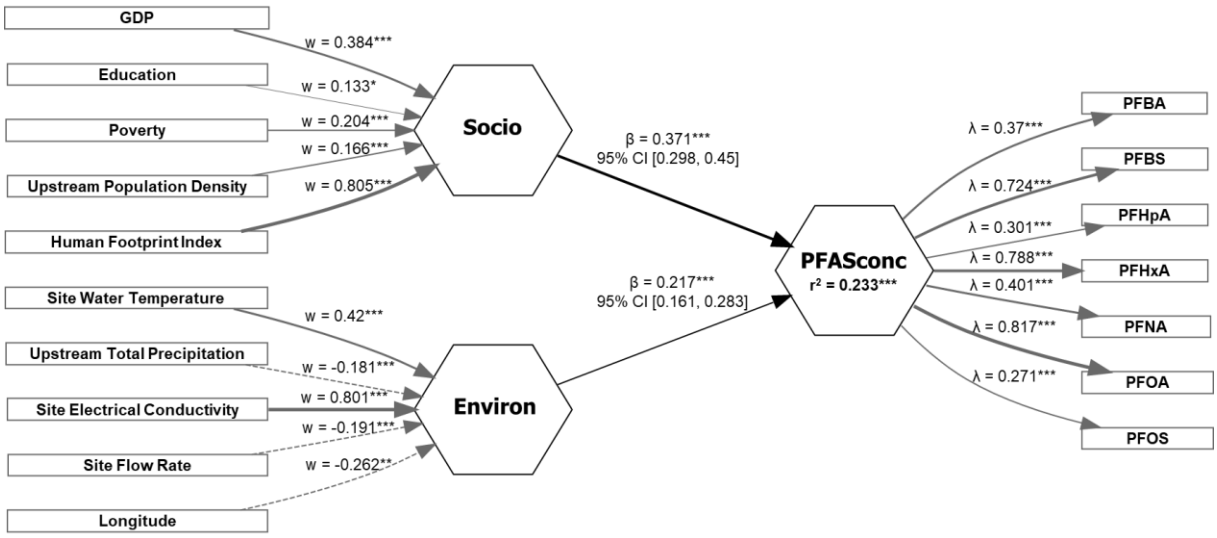

Figure 3. PLS-PM model of socioeconomic and environmental factors influencing PFAS concentration in European rivers. 'Socio,' 'Environ,' and 'PFASconc' represent the latent variables (LVs) for 'socioeconomic variables,' 'environmental variables,' and the dependent variable ('PFAS concentration'), respectively. 'w,' 'β,' and 'λ' represent the weights of individual variables, the path coefficients of latent variables, and the loadings of manifest variables on their corresponding latent variables, respectively. r^2, the coefficient of determination, indicates the amount of variance in a dependent latent variable explained by its independent latent variables.

Electrical conductivity (weight = 0.801, $p < 0.001$) was the most significant environmental variable positively associated with PFAS concentrations, likely due to its co-occurrence with dissolved ions from wastewater effluents or industrial discharges, suggesting they may share anthropogenic origins or similar transport mechanisms in aquatic environments. Regional temperature variations (weight = 0.420, $p < 0.001$) were also identified as a potential driver, potentially due to higher temperatures increasing the volatility of some PFAS compounds (e.g. PFBA and PFBS) and accelerating the degradation of precursors (potentially leading to higher levels of PFHxA and PFBA). Longitude showed a significant negative relationship (weight = –0.262, $p < 0.01$), suggesting that PFAS concentrations were generally higher in western Europe and declined towards the east, possibly reflecting regional differences in industrialisation, consumption patterns, and regulatory implementation. Regional precipitation (weight = -0.181, $p < 0.001$) and flow rate (weight = -0.191, $p < 0.001$) were also identified as potential drivers, likely due to dilution effects (Kwok et al., 2010; Nguyen et al., 2022; Lee et al., 2020). Taken together, the analysis indicates that spatial variations in the occurrence of PFAS in European surface waters result from the complex dynamics of interactions between human activities and environmental factors.

3.6 Implications of our findings for ecological and human health

Threshold values have been proposed for combinations of PFAS and for PFOS for surface waters and drinking water (European Union, 2013; European Union, 2020; European Commission, 2022). The EU has proposed an annual average Environmental Quality Standard (EQS) of 4.4 ng/L for the sum of 24 PFAS in surface waters, seven of which were monitored in this study (European Commission, 2022), and an individual annual average EQS of 0.65 ng/L for PFOS (European Union, 2013). The EU have also proposed a threshold value of 100 ng/L for the sum of 20 PFAS in drinking water to protect human health (European Union,

2020). Overall, 63% of the monitored locations had an annual average PFAS concentration exceeding the AA-EQS of 4.4 ng/L for the sum of 24 PFAS compounds (Figure 4 and Figure S2). The greatest level of exceedances of the AA-EQS was seen for the site on the Garyllis River in Cyprus (92 times the EQS), the two sites on the River Kelvin in Scotland (23.8 and 23 times the EQS), and the site on the River Almond in Scotland (22 times the EQS). Only 2.0% of samples had annual average concentrations of PFOS higher than the AA-EQS for EU surface waters (Figure S2). The sites with the highest exceedance of the PFOS AA-EQS (0.65 ng/L) were all in Germany on the Aller River (including two sites, 104 and 85 times the EQS), the Mühlengraben River (26 times EQS) and the Tarpenbek River (21 times EQS). This exceedance rate is considerably lower than recent European Environment Agency data (EEA, 2024b), which report that 50–60% of river monitoring sites across Europe (out of 386 to 1,097 sites annually) exceeded the EQS between 2018 and 2022. The lower exceedance rate observed in our study may partly underestimate the true extent of PFOS exceedances, as the AA-EQS threshold of 0.65 ng/L falls below the method detection limit (1.76 ng/L) used in this study. Around 2.5% of the samples exceeded the EU threshold of 100 ng/L for the sum of 20 PFAS in drinking water (Figure S2). In contrast, a larger proportion of samples exceeded US EPA drinking water limits: 29% of samples exceeded the 4 ng/L limit for PFOA, 2.7% exceeded the 10 ng/L limit for PFNA, and 1.0% exceeded the 4 ng/L limit for PFOS. These findings indicate that exceedances are substantially more frequent when assessed against the US EPA thresholds. Given that we only looked at seven PFAS and the surface water and drinking water thresholds are based on 20 and 24 different PFAS respectively, true exceedance rates are likely underestimated.

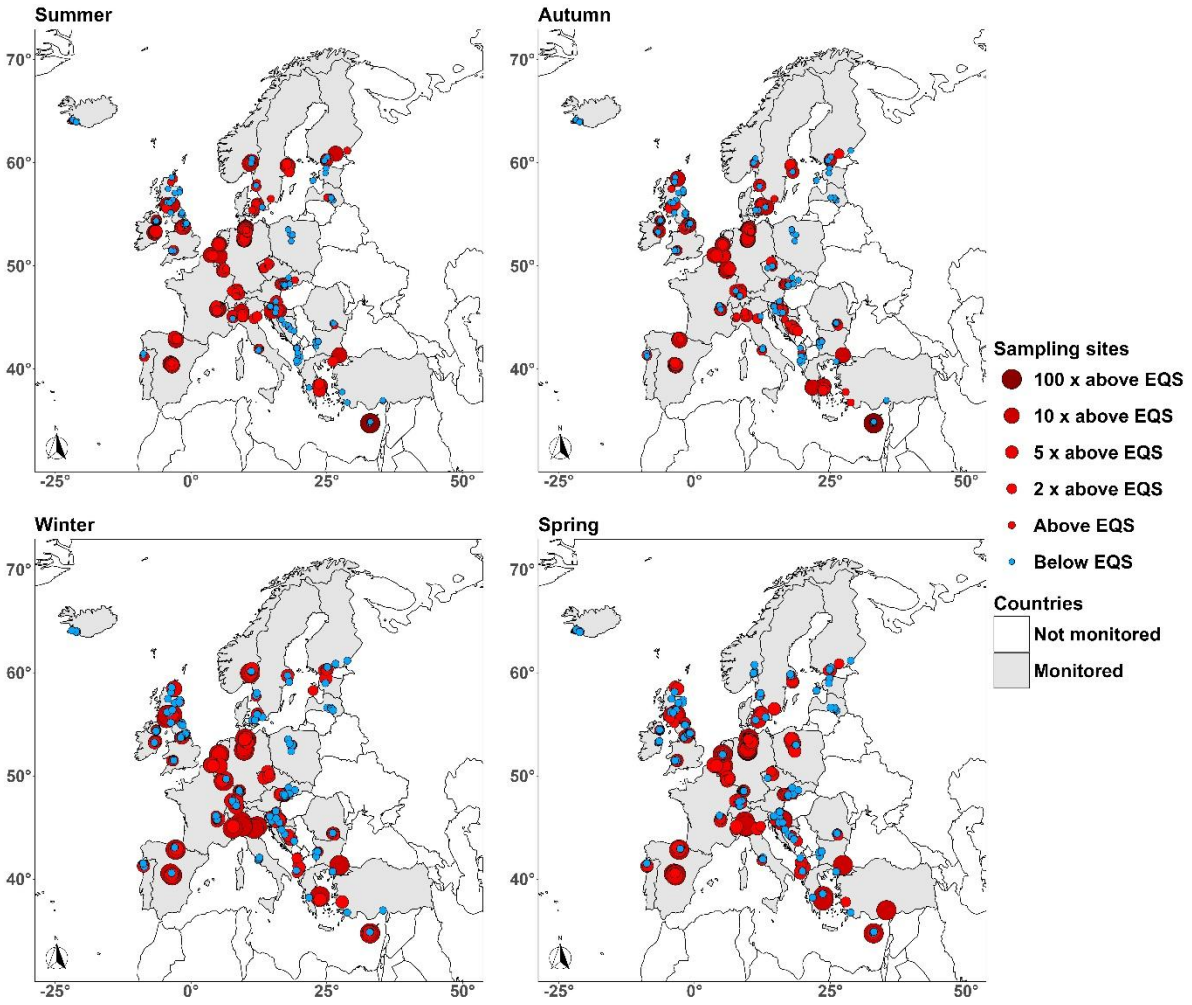

Figure 4. Comparison of the annual average sum of PFAS concentrations for the different monitoring locations with the annual average PFAS Environmental Quality Standard for EU surface water. Blue points are below the EQS. Red points are greater than the EQS with the size indicating the level of exceedance.

3.7 Final considerations

This comprehensive study provides an unprecedented large-scale assessment of PFAS contamination across European freshwater systems and reveals important insights into their spatial and temporal distribution and the key drivers influencing their presence. Our findings underscore the pervasive nature of these chemicals, with detections in all 31 countries monitored. The identification of wastewater treatment plants, landfills, and recycling centres as significant sources of pollution, coupled with the strong association between PFAS concentrations and socioeconomic indicators like the Human Footprint Index and GDP, highlights the intertwined relationship between human activity and environmental contamination. The observed seasonal variations further emphasize the complex dynamics governing PFAS distribution, pointing to factors such as dilution, human activity, and the transformation of precursor substances as drivers of exposure.

The widespread exceedance of established environmental quality standards for PFAS at 63% of European sites, even with a limited set of seven compounds, presents a stark picture of the ecological and health hazards posed by these substances. This study serves as a crucial foundation for understanding the continent-wide challenge posed by PFAS. The insights gained are invaluable for informing and strengthening regulatory frameworks, guiding targeted mitigation strategies, and prioritizing areas for remediation efforts. Future research should aim to expand the suite of PFAS monitored, further investigate the long-term environmental fate and transport of these compounds, and explore innovative solutions for their removal from aquatic environments. Ultimately, a concerted, international effort is essential to curb PFAS pollution and safeguard both ecosystem integrity and public health across Europe and beyond.

Reference

Key, B. D., Howell, R. D., & Criddle, C. S. (1997). Fluorinated organics in the biosphere. *Environmental science & technology*, *31*(9), 2445-2454.

Buck, R. C., Franklin, J., Berger, U., Conder, J. M., Cousins, I. T., De Voogt, P., & van Leeuwen, S. P. (2011). Perfluoroalkyl and polyfluoroalkyl substances in the environment: terminology, classification, and origins. *Integrated environmental assessment and management*, *7*(4), 513-541.

Cousins, I. T., DeWitt, J. C., Glüge, J., Goldenman, G., Herzke, D., Lohmann, R., & Wang, Z. (2020). The high persistence of PFAS is sufficient for their management as a chemical class. *Environmental Science: Processes & Impacts*, *22*(12), 2307-2312.

494 Shi, Y., Vestergren, R., Xu, L., Song, X., Niu, X., Zhang, C., & Cai, Y. (2015). Characterizing
495 direct emissions of perfluoroalkyl substances from ongoing fluoropolymer production sources:
496 A spatial trend study of Xiaoqing River, China. *Environmental pollution*, *206*, 104-112.

497

498 Chen, H., Sun, R., Zhang, C., Han, J., Wang, X., Han, G., & He, X. (2016). Occurrence, spatial
499 and temporal distributions of perfluoroalkyl substances in wastewater, seawater and sediment
500 from Bohai Sea, China. *Environmental pollution*, *219*, 389-398.

501

502 Camacho, C. G., Antonison, A., Oldnettle, A., Costa, K. A., Timshina, A. S., Ditz, H., ... &
503 Bowden, J. A. (2024). Statewide Surveillance and Mapping of PFAS in Florida Surface Water.
504 *ACS ES&T Water*, *4*(10), 4343-4355.

505

506 Becker, A. M., Gerstmann, S., & Frank, H. (2008). Perfluorooctane surfactants in waste waters,
507 the major source of river pollution. *Chemosphere*, *72*(1), 115-121.

508

509 Reinikainen, J., Perkola, N., Äystö, L., & Sorvari, J. (2022). The occurrence, distribution, and
510 risks of PFAS at AFFF-impacted sites in Finland. *Science of the Total Environment*, *829*,
511 154237.

512

513 Pizzurro, D. M., Seeley, M., Kerper, L. E., & Beck, B. D. (2019). Interspecies differences in
514 perfluoroalkyl substances (PFAS) toxicokinetics and application to health-based criteria.
515 *Regulatory Toxicology and Pharmacology*, *106*, 239-250.

516

517 Messmer, M. F., Salloway, J., Shara, N., Locwin, B., Harvey, M. W., & Traviss, N. (2022). Risk
518 of cancer in a community exposed to per-and poly-fluoroalkyl substances. *Environmental*
519 *health insights*, *16*, 11786302221076707.

520

521 Sinclair, G. M., Long, S. M., & Jones, O. A. (2020). What are the effects of PFAS exposure at
522 environmentally relevant concentrations?. *Chemosphere*, *258*, 127340.

523

524 Wang, L., Yang, T., Liu, X., Liu, J., & Liu, W. (2024). Critical evaluation and meta-analysis of
525 ecotoxicological data on per-and polyfluoroalkyl substances (PFAS) in freshwater species.
526 *Environmental Science & Technology*, *58*(40), 17555-17566.

527

528 European Union, 2013. Directive 2013/39/EU of the European Parliament and of the Council
529 of 12 August 2013 amending Directives 2000/60/EC and 2008/105/EC as regards priority
530 substances in the field of water policy. Official Journal of the European Union L226:1–17.

531

532 European Commission, 2022. ANNEXES to the Proposal for a Directive of the European
533 Parliament and of the Council amending Directive 2000/60/EC establishing a framework for
534 Community action in the field of water policy, Directive 2006/118/EC on the protection of
535 groundwater against pollution and deterioration and Directive 2008/105/EC on environmental
536 quality standards in the field of water policy. COM (2022) 540 final.
537 https://environment.ec.europa.eu/publications/p roposal-amending-water-directives_en.

538

539 U.S. Environmental Protection Agency (US EPA), 2023. Per- and Polyfluoroalkyl Substances
540 (PFAS) Proposed PFAS National Primary Drinking Water Regulation; https://www.
541 epa.gov/sdwa/and-polyfluoroalkyl-substances-pfas.

542

543 European Union. 2020, Directive (EU) 2020/2184 of the European Parliament and of the
544 Council of 16 December 2020 on the quality of water intended for human consumption
545 (recast). Official Journal of the European Union L 435/1.

546

547 Zarębska, M., Bajkacz, S., & Hordyjewicz-Baran, Z. (2024). Assessment of legacy and
548 emerging PFAS in the Oder River: Occurrence, distribution, and sources. *Environmental*
549 *Research*, *251*, 118608.

550

551 Sörengård, M., Bergström, S., McCleaf, P., Wiberg, K., & Ahrens, L. (2022). Long-distance
552 transport of per-and polyfluoroalkyl substances (PFAS) in a Swedish drinking water aquifer.
553 *Environmental Pollution*, *311*, 119981.

554

555 Jonker, M. T. (2024). Per-and Polyfluoroalkyl Substances in Water (2008–2022) and Fish
556 (2015–2022) in The Netherlands: Spatiotemporal Trends, Fingerprints, Mass Discharges,
557 Sources, and Bioaccumulation Factors. *Environmental Toxicology and Chemistry*, 43(5), 965-
558 975.

559

560 Pan, Y., Zhang, H., Cui, Q., Sheng, N., Yeung, L. W., Sun, Y., & Dai, J. (2018). Worldwide
561 distribution of novel perfluoroether carboxylic and sulfonic acids in surface water.
562 *Environmental science & technology*, *52*(14), 7621-7629.

563

564 Baabish, A., Sobhanei, S., & Fiedler, H. (2021). Priority perfluoroalkyl substances in surface
565 waters-a snapshot survey from 22 developing countries. *Chemosphere*, *273*, 129612.

566

567 Loos, R., Gawlik, B. M., Locoro, G., Rimaviciute, E., Contini, S., & Bidoglio, G. (2009). EU-
568 wide survey of polar organic persistent pollutants in European river waters. *Environmental*
569 *pollution*, *157*(2), 561-568.

570

Ackerman Grunfeld, D., Gilbert, D., Hou, J., Jones, A. M., Lee, M. J., Kibbey, T. C., & O'Carroll, D. M. (2024). Underestimated burden of per-and polyfluoroalkyl substances in global surface waters and groundwaters. *Nature Geoscience*, *17*(4), 340-346.

Cordner, A., Brown, P., Cousins, I. T., Scheringer, M., Martinon, L., Dagorn, G., & Horel, S. (2024). PFAS contamination in Europe: generating knowledge and mapping known and likely contamination with "expert-reviewed" journalism. *Environmental Science & Technology*, *58*(15), 6616-6627.

Niegowska, M., Pretto, P., Porcel-Rodriguez, E., Marinov, D., Ceriani, L., & Lettieri, T. (2021). *Per-and polyfluoroalkyl substances (PFAS) of possible concern in the aquatic environment*. Publications Office of the European Union.

Wilkinson, J. L., Boxall, A. B., Kolpin, D. W., Leung, K. M., Lai, R. W., Galbán-Malagón, C., & Teta, C. (2022). Pharmaceutical pollution of the world's rivers. *Proceedings of the National Academy of Sciences*, *119*(8), e2113947119.

Wilkinson, J. L., Boxall, A. B., & Kolpin, D. W. (2019). A novel method to characterise levels of pharmaceutical pollution in large-scale aquatic monitoring campaigns. *Applied Sciences*, *9*(7), 1368.

Antweiler, R. C. (2015). Evaluation of statistical treatments of left-censored environmental data using coincident uncensored data sets. II. Group comparisons. *Environmental Science & Technology*, *49*(22), 13439-13446.

Eurostat. (2024). *Glossary: Nomenclature of territorial units for statistics (NUTS)*, European Commission. Retrieved October 2024, from https://ec.europa.eu/eurostat/statistics-explained/index.php?title=Glossary:Nomenclature_of_territorial_units_for_statistics_(NUTS).

European Environment Agency (EEA), 2024a. Industrial Reporting under the Industrial Emissions Directive 2010/75/EU and European Pollutant Release and Transfer Register Regulation (EC) No. 166/2006. Prod-ID: DAT-238-en, DAT-149-en. Published 12 September 2024, last modified 4 December 2024. Available at: https://www.eea.europa.eu/en/datahub/datahubitem-view/9405f714-8015-4b5b-a63c-280b82861b3d.

Ehalt Macedo, H., Lehner, B., Nicell, J., Grill, G., Li, J., Limtong, A., & Shakya, R. (2022). Distribution and characteristics of wastewater treatment plants within the global river network. *Earth System Science Data*, *14*(2), 559-577.

Mu, H., Li, X., Wen, Y., Huang, J., Du, P., Su, W., & Geng, M. (2022). A global record of annual terrestrial Human Footprint dataset from 2000 to 2018. *Scientific Data*, *9*(1), 176.

Lehner, B., & Grill, G. (2013). Global river hydrography and network routing: baseline data and new approaches to study the world's large river systems. *Hydrological Processes*, *27*(15), 2171-2186.

Salminen R., Batista, M.J., Bidovec, M., Demetriades, A., De Vivo, B., De Vos, W., Duris, M., Gilucis, A., Gregorauskiene, V., Halamic, J., Heitzmann, P., Lima, A., Jordan, G., Klaver, G., Klein, P., Lis, J., Locutura, J., Marsina, K., Mazreku, A., O'Connor, P.J., Olsson, S.Å., Ottesen, R.T., Petersell, V., Plant, J.A., Reeder, S., Salpeteur, I., Sandström, H., Siewers, U., Steenfelt, A. Tarvainen, T. 2005. FOREGS Geochemical Atlas of Europe, Part 1: Background Information, Methodology and Maps. Geological Survey of Finland, Espoo.

Abatzoglou, J. T., Dobrowski, S. Z., Parks, S. A., & Hegewisch, K. C. (2018). TerraClimate, a high-resolution global dataset of monthly climate and climatic water balance from 1958–2015. *Scientific data*, *5*(1), 1-12.

Barbarossa, V., Huijbregts, M. A., Beusen, A. H., Beck, H. E., King, H., & Schipper, A. M. (2018). FLO1K, global maps of mean, maximum and minimum annual streamflow at 1 km resolution from 1960 through 2015. *Scientific Data*, *5*(1), 1-11.

European Union, 2006. Directive 2006/122/EC of the European parliament and of the council of 12. Off. J. Eur. Union L 372/32, 32–34. https://eur-lex.europa.eu/LexUriServ/LexUriServ.do?uri=OJ:L:2006:372:0032:0034:en:PDF.

European Commission, 2017. Commission Regulation (EU) 2017/1000 of 13 June 2017 amending Annex XVII to Regulation (EC) No 1907/2006 of the European Parliament and of the Council concerning the Registration, Evaluation, Authorisation and Restriction of Chemicals (REACH) as regards perfluorooctanoic acid (PFOA), its salts and PFOA-related substances. *Official Journal of the European Union*, L 150, 14 June 2017, pp. 14–18. Available at: https://eur-lex.europa.eu/eli/reg/2017/1000/oj.

Fernandez, N., Nejadhashemi, A. P., & Loveall, C. (2023). Large-scale assessment of PFAS compounds in drinking water sources using machine learning. *Water Research*, *243*, 120307.

Zhao, L., Chen, J., Wen, J., Li, Y., Zhang, Y., Wu, Q., & Yu, G. (2025). Unveiling PFAS hazard in European surface waters using an interpretable machine-learning model. *Environment International*, 109504.

Munoz, G., Giraudel, J. L., Botta, F., Lestremau, F., Dévier, M. H., Budzinski, H., & Labadie, P. (2015). Spatial distribution and partitioning behavior of selected poly-and perfluoroalkyl

652 substances in freshwater ecosystems: a French nationwide survey. *Science of the Total*
653 *Environment*, *517*, 48-56.

654

655 Pignotti, E., Casas, G., Llorca, M., Tellbüscher, A., Almeida, D., Dinelli, E., & Barceló, D.
656 (2017). Seasonal variations in the occurrence of perfluoroalkyl substances in water, sediment
657 and fish samples from Ebro Delta (Catalonia, Spain). *Science of the Total Environment*, *607*,
658 933-943.

659

660 Podder, A., Sadmani, A. A., Reinhart, D., Chang, N. B., & Goel, R. (2021). Per and poly-
661 fluoroalkyl substances (PFAS) as a contaminant of emerging concern in surface water: A
662 transboundary review of their occurrences and toxicity effects. *Journal of hazardous materials*,
663 *419*, 126361.

664

665 Bertilsson, S., Burgin, A., Carey, C. C., Fey, S. B., Grossart, H. P., Grubisic, L. M., & Smyth,
666 R. L. (2013). The under-ice microbiome of seasonally frozen lakes. *Limnology and*
667 *Oceanography*, *58*(6), 1998-2012.

668

669 Zhao, L., Zhou, M., Zhang, T., & Sun, H. (2013). Polyfluorinated and perfluorinated chemicals
670 in precipitation and runoff from cities across eastern and central China. *Archives of*
671 *environmental contamination and toxicology*, *64*, 198-207.

672

673 Wang, N., Szostek, B., Buck, R. C., Folsom, P. W., Sulecki, L. M., & Gannon, J. T. (2009). 8-2
674 Fluorotelomer alcohol aerobic soil biodegradation: Pathways, metabolites, and metabolite
675 yields. *Chemosphere*, *75*(8), 1089-1096.

676

677 Shaw, D. M., Munoz, G., Bottos, E. M., Duy, S. V., Sauvé, S., Liu, J., & Van Hamme, J. D.
678 (2019). Degradation and defluorination of 6: 2 fluorotelomer sulfonamidoalkyl betaine and 6:
679 2 fluorotelomer sulfonate by Gordonia sp. strain NB4-1Y under sulfur-limiting conditions.
680 *Science of the Total Environment*, *647*, 690-698.

681

682 Calore, F., Guolo, P. P., Wu, J., Xu, Q., Lu, J., & Marcomini, A. (2023). Legacy and novel
683 PFASs in wastewater, natural water, and drinking water: Occurrence in Western Countries vs
684 China. *Emerging Contaminants*, *9*(3), 100228.

685

686 Zhang, W., Zhang, Y., Taniyasu, S., Yeung, L. W., Lam, P. K., Wang, J., & Dai, J. (2013).
687 Distribution and fate of perfluoroalkyl substances in municipal wastewater treatment plants in
688 economically developed areas of China. *Environmental pollution*, *176*, 10-17.

689

690 Ayodele, A., & Obeng-Gyasi, E. (2024). Exploring the potential link between PFAS exposure
691 and endometrial cancer: A review of environmental and sociodemographic factors. *Cancers*,
692 *16*(5), 983.

693

694 Lee, Y. M., Lee, J. Y., Kim, M. K., Yang, H., Lee, J. E., Son, Y., & Zoh, K. D. (2020).
695 Concentration and distribution of per-and polyfluoroalkyl substances (PFAS) in the Asan Lake
696 area of South Korea. *Journal of hazardous materials*, *381*, 120909.

697

698 Kwok, K. Y., Taniyasu, S., Yeung, L. W., Murphy, M. B., Lam, P. K., Horii, Y., & Yamashita, N.
699 (2010). Flux of perfluorinated chemicals through wet deposition in Japan, the United States,
700 and several other countries. *Environmental science & technology*, *44*(18), 7043-7049.

701

702 Nguyen, M. A., Norström, K., Wiberg, K., Gustavsson, J., Josefsson, S., & Ahrens, L. (2022).
703 Seasonal trends of per-and polyfluoroalkyl substances in river water affected by fire training
704 sites and wastewater treatment plants. *Chemosphere*, *308*, 136467.

705

706 European Environment Agency (EEA), 2024b. *PFAS pollution in European waters.* Published
707 9 December 2024. Available at: https://www.eea.europa.eu/en/analysis/publications/pfas-
708 pollution-in-european-waters.

709